

Effects of Substituents and Solvents on the Reactions of Iminophosphorane with Formaldehyde: *Ab Initio* MO Calculation and Monte Carlo Simulation

Ying Xue and Chan Kyung Kim*

Department of Chemistry, Inha University, Incheon 402-751, Korea

Received: May 20, 2003; In Final Form: August 4, 2003

Ab initio molecular orbital method and Monte Carlo (MC) simulation with free energy perturbation (FEP) techniques have been used to study the aza-Wittig reaction of iminophosphoranes ($\text{H}_3\text{P}=\text{NH}$) with formaldehyde (H_2CO) in the gas phase and in three different solvents: water, methanol, and tetrahydrofuran (THF). The optimized structures and thermodynamic properties of stationary points for the title reaction system in the gas phase were calculated at the MP2/6-31G** level of theory. The effects of substituents on the reactivity of iminophosphorane were discussed. This aza-Wittig reaction is more favorable for $\text{X}=\text{H}$ and CH_3 than for $\text{X}=\text{Cl}$ in the gas phase. The potential energy profiles along the minimum energy path in the gas phase and in three solvents were obtained. The solvent effects on the $\text{H}_3\text{P}=\text{NH} + \text{H}_2\text{CO}$ reaction increase in the order water \approx methanol $>$ THF, suggesting that the protic polar solvents are more suitable for the aza-Wittig reaction.

1. Introduction

The Wittig reaction of methylenephosphorane with a carbonyl compound is one of the most important organic transformations and was extensively investigated via both experimental and theoretical methods.^{1–10} In the past, the structures and reactions of iminophosphoranes were the focus because of their similarity with methylenephosphoranes. As the isoelectronic molecules of methylenephosphoranes, iminophosphoranes were proven to have versatile properties and to undergo a series of interesting chemical reactions.^{11–15} Several *ab initio* calculations have been carried out to explore the electronic properties of iminophosphoranes and the mechanism of the aza-Wittig reaction, the reaction of iminophosphoranes with carbonyl compounds.^{16–20} The first results of *ab initio* calculation at the MP2/D2-d level on the aza-Wittig reaction of iminopnictoranes ($\text{H}_3\text{M}=\text{NH}$, $\text{M}=\text{P}$, As , Sb , and Bi) with H_2CO in the gas phase were reported by Koketsu *et al.*¹⁷ in 1997, where this reaction was found to be a stepwise process for any pnicogen. For M , the attacking of atoms C and O in H_2CO to atoms N and M in $\text{H}_3\text{M}=\text{NH}$, respectively, forms a four-membered ring intermediate (INT1) via transition state TS1; then the trigonal bipyramidal M of INT1 undergoes a pseudorotation to form another four-membered cyclic structure (INT2) with ~ 2 – 5 kcal/mol more energy than INT1. INT2 has one imaginary frequency and is the pseudorotational transition state at the M center. The final step corresponds to the cycloreversion of INT2 to yield $\text{H}_2\text{C}=\text{NH}$ and $\text{H}_3\text{M}=\text{O}$ through transition state TS2. Lu *et al.*¹⁸ studied another aza-Wittig reaction, the reaction of $\text{X}_3\text{P}=\text{NH}$ ($\text{X}=\text{Cl}$, H , or CH_3) with $\text{O}=\text{CHCOOH}$ using the MP2/6-31G** method at the HF/6-31G**-optimized structures. They also obtained two similar intermediates when $\text{X}=\text{H}$ and Cl (when $\text{X}=\text{CH}_3$, there is only one intermediate) at the HF/6-31G** level. But they pointed out that these two intermediates would become accurately one minimum when the MP2/6-31G** method was used in the structure optimization. In our previous study,²⁰ we

performed *ab initio* calculations at the MP2/6-31G** level of theory for the reactions of $\text{X}_3\text{P}=\text{NH}$ with H_2CO ($\text{X}=\text{H}$ or Cl) to examine the identity of INT1 and INT2 and to gain some information about these reactions in the gas phase. We found that the aza-Wittig reaction proceeds in two steps. The first step is the formation of a four-membered cyclic intermediate (INT) via transition state TS1 from the dipole–dipole complex (RC) of iminophosphorane and H_2CO , and the second step is opening of the ring intermediate to yield a complex (PC) of $\text{H}_2\text{C}=\text{NH}$ and the phosphorus oxide $\text{H}_3\text{P}=\text{O}$ via transition state TS2 (see Scheme 1).

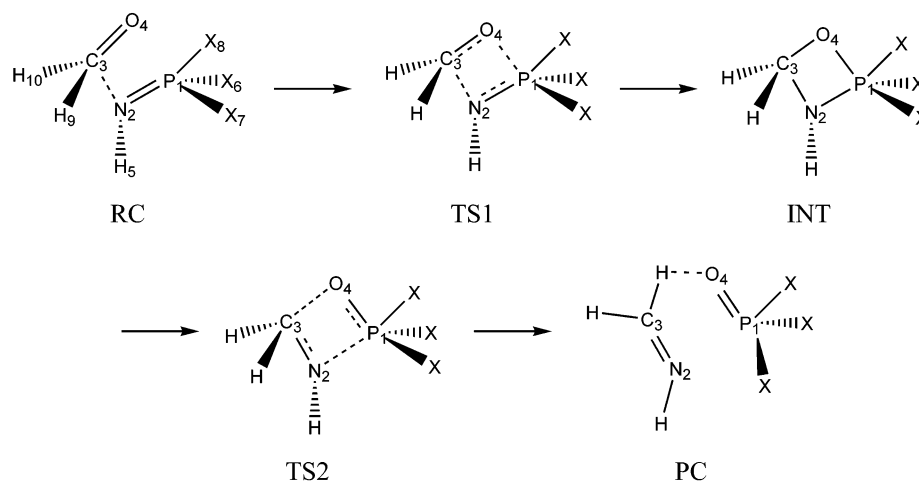
This work follows our earlier study²⁰ and focuses on the details, including stereochemistry, substituent, and solvation effects in three different solvents for the aza-Wittig reaction of $\text{H}_3\text{P}=\text{NH}$ with H_2CO . The changes in the thermodynamic and kinetic properties caused by replacement of three hydrogen atoms on atom P with CH_3 and Cl substituents, respectively, are explored. Finally, the effects of water, methanol, and tetrahydrofuran (THF) as solvents will be studied using the Monte Carlo free energy perturbation method.

2. Computational Details

2.1. Gas Phase Calculation. The geometric structures of all the reactant complexes (RC), product complexes (PC), intermediates (INT), and transition states (TS1 and TS2) of the $\text{X}_3\text{P}=\text{NH}$ and $\text{H}_2\text{C}=\text{O}$ reaction systems ($\text{X}=\text{CH}_3$, H , and Cl) (Scheme 1) were optimized at the second-order Møller–Plesset perturbation level with the 6-31G** basis set (MP2/6-31G**). The nature of the stationary points was confirmed by the harmonic frequency analysis as a minimum with all positive frequencies or as a transition state with only one imaginary frequency. Three minima (RC, INT, and PC) and two transition states (TS1 and TS2) were obtained. The frequency calculations at the MP2/6-31G** level without scaling also provided the thermodynamic quantities such as the zero-point vibrational energy, thermal correction, enthalpies, Gibbs free energies, and entropies at 298.15 K and 1 atm.

* To whom correspondence should be addressed. E-mail: kkyung@inha.ac.kr. Telephone: +82-32-860-7684. Fax: +82-32-867-5604.

SCHEME 1



The intrinsic reaction coordinate (IRC) calculations²¹ were performed to verify the connections between RC and INT through TS1 as well as between INT and PC through TS2. In the IRC calculations for the $\text{H}_3\text{P}=\text{NH} + \text{H}_2\text{CO}$ reaction system, the “IRC=tight” option was used to generate the minimum energy path (MEP) in the gas phase. The MEPs at the MP2/6-31G** level were constructed with a step size of $0.05 \text{ amu}^{1/2}$ bohr for a total of 87 steps in both directions from TS1 and with a step size of $0.10 \text{ amu}^{1/2}$ bohr for a total of 115 steps in both directions from TS2. The partial charges were calculated for all points along the MEP using the CHELPG method²² and at the MP2/6-31G** level of theory. All *ab initio* molecular orbital calculations were carried out using Gaussian 98.²³

2.2. Monte Carlo Simulation. For the reaction path obtained by *ab initio* MO calculation, those geometries and partial charges along the MEP were incorporated into a molecular mechanical potential for the reaction system immersed in a periodic box of explicit solvent molecules and used to calculate free energy changes of solvation along the MEP by the Monte Carlo simulation method. The intermolecular interaction potential function for the solute–solvent and solvent–solvent interactions was described by Coulomb and Lennard-Jones (LJ) terms between atom *i* in molecule a and atom *j* in molecule b, which are separated by a distance r_{ij} as shown in eq 1.

$$\Delta E_{ab} = \sum \sum \{q_i q_j e^2 / r_{ij} + 4\epsilon_{ij} (\sigma_{ij} / r_{ij})^{12} - (\sigma_{ij} / r_{ij})^6\} \quad (1)$$

The crossing terms were obtained by the combination rules:

$$\epsilon_{ij} = (\epsilon_{ii} \epsilon_{jj})^{1/2}, \quad \sigma_{ij} = (\sigma_{ii} \sigma_{jj})^{1/2} \quad (2)$$

No intramolecular terms were included. The ϵ and σ constants for the solute were taken from the OPLS all-atom parameters of the BOSS 4.2²⁴ database. q_i is the partial charge of atom *i* obtained in the above gas phase calculation. In this study, we have used three solvents, water (TIP4P model), methanol, and THF. The reacting system as a solute was solvated in boxes containing 396 molecules of H_2O , CH_3OH , and THF, which had dimensions of approximately $20 \text{ \AA} \times 20 \text{ \AA} \times 30 \text{ \AA}$, $26.7 \text{ \AA} \times 26.7 \text{ \AA} \times 40.0 \text{ \AA}$, and $32.5 \text{ \AA} \times 32.5 \text{ \AA} \times 48.8 \text{ \AA}$, respectively. For the solvent, the OPLS united-atom models were adopted and the parameters also taken from the BOSS 4.2 database.

The changes in the free energy of solvation along the MEP were calculated by Monte Carlo simulation with statistical perturbation theory.²⁵ Preferential sampling was used in the

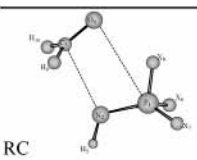
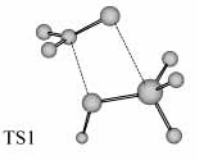
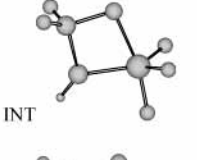
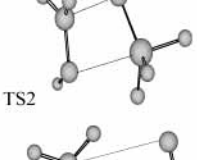
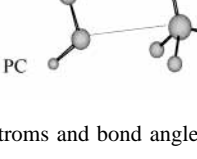
Metropolis algorithm, and the perturbations were carried out using double-wide sampling in 22 windows for step 1 and 23 windows for step 2 of the aza-Wittig reaction in each solvent. Every simulation involved 2×10^6 configurations for equilibration, followed by 4×10^6 configurations of averaging in the isothermal, isobaric (NPT) ensemble at 298.15 K and 1 atm. A cutoff of 10.0 for solute–solvent and solvent–solvent interaction was used for each solvent. All Monte Carlo simulation calculations were performed using BOSS 4.2.²⁴ To obtain the total potential energy profile along the reaction path in solution, the gas phase relative energies were added to the computed free energy changes of solvation.

3. Results and Discussion

3.1. Substituent Effects in the Gas Phase. The structures of the aza-Wittig $\text{H}_3\text{P}=\text{NH} + \text{H}_2\text{CO}$ reaction system were optimized at the MP2/6-31G** level of theory, and it was found that this reaction is a two-step process. We replaced three hydrogen atoms at the P atom with CH_3 and Cl groups, and the equilibrium geometries of all stationary points of the reaction systems ($\text{X}_3\text{P}=\text{NH} + \text{H}_2\text{CO}$, X = CH_3 and Cl) were obtained at the MP2/6-31G** level. It was observed that the reaction mechanism of the reaction systems ($\text{X}_3\text{P}=\text{NH} + \text{H}_2\text{CO}$) when X = CH_3 and Cl is similar to that when X = H. That is, there are also three minima, reaction complex (RC), intermediate (INT), and product complex (PC), and two transition states, TS1 and TS2, on the potential energy surface. The main optimized geometrical parameters of all stationary points along the reaction path are given in Table 1 for the reaction of $\text{X}_3\text{P}=\text{NH}$ (X = CH_3 , H, and Cl) with H_2CO .

When X = H, the structure of transition state TS1 of the aza-Wittig reaction has breaking $\text{P}_{(1)}-\text{N}_{(2)}$ and $\text{C}_{(3)}-\text{O}_{(4)}$ bond distances of 1.609 and 1.258 Å, respectively, and forming $\text{N}_{(2)}-\text{C}_{(3)}$ and $\text{P}_{(1)}-\text{O}_{(4)}$ bond distances of 1.963 and 2.434 Å, respectively. The Cl substituent at the $\text{P}_{(1)}$ position slightly shortens the $\text{P}_{(1)}-\text{N}_{(2)}$ bond by 0.014 Å and the $\text{P}_{(1)}-\text{O}_{(4)}$ bond by 0.092 Å, and has a negligible influence on the $\text{N}_{(2)}-\text{C}_{(3)}$ and $\text{C}_{(3)}-\text{P}_{(1)}$ bond distances. The methyl group substituted at $\text{P}_{(1)}$ causes much lengthening of the $\text{P}_{(1)}-\text{N}_{(2)}$, $\text{P}_{(1)}-\text{O}_{(4)}$, and $\text{C}_{(3)}-\text{O}_{(4)}$ bonds in the TS1 structure. The steric effect of three CH_3 groups would prohibit the O atom of the formaldehyde from approaching the P atom. For transition state TS2, the bond lengths of the breaking $\text{P}_{(1)}-\text{N}_{(2)}$ and $\text{C}_{(3)}-\text{O}_{(4)}$ bonds in the $\text{H}_3\text{P}=\text{NH} + \text{H}_2\text{CO}$ reaction system are 2.244 and 1.834 Å, respectively. The $\text{N}_{(2)}-\text{C}_{(3)}$ and $\text{P}_{(1)}-\text{O}_{(4)}$ bond distances are 1.335 and 1.572 Å, respectively, and become shorter by 0.017

TABLE 1: Selected Geometric Parameters Optimized at the MP2/6-31G** Level of Theory for the Aza-Wittig Reaction^a

	X	P ₁ N ₂	N ₂ C ₃	C ₃ O ₄	P ₁ O ₄	P ₁ N ₂ C ₃	N ₂ C ₃ O ₄	PNCO
 RC	CH ₃	1.589	2.691	1.227	3.487	102.9	109.9	6.3
	H	1.577	2.674	1.224	3.359	104.1	103.4	0.0
	Cl	1.541	2.943	1.221	3.675	103.4	105.2	23.3
 TS1	CH ₃	1.633	1.752	1.283	2.735	108.7	109.8	-5.4
	H	1.609	1.963	1.258	2.434	98.8	99.1	0.0
	Cl	1.595	1.966	1.259	2.342	97.1	95.6	-15.6
 INT	CH ₃	1.708	1.460	1.403	1.841	96.5	96.0	-9.5
	H	1.689	1.463	1.410	1.787	95.5	95.2	-7.9
	Cl	1.653	1.453	1.426	1.725	95.7	93.8	0.1
 TS2	CH ₃	2.364	1.349	1.720	1.594	80.3	104.6	12.4
	H	2.244	1.335	1.834	1.572	83.8	101.3	12.3
	Cl	2.020	1.318	1.997	1.554	93.4	89.7	17.6
 PC	CH ₃	3.707	1.285	3.222	1.512	86.0	97.1	0.0
	H	3.034	1.284	3.105	1.502	103.0	81.3	0.0
	Cl	3.238	1.282	3.132	1.478	106.3	76.8	0.0

^a Bond lengths in angstroms and bond angles in degrees.

TABLE 2: Changes in Electronic Energies, Zero-Point Vibration Energy Corrections, Enthalpies, and Gibbs Free Energies for All Steps in the Aza-Wittig Reactions of X₃P=NH with H₂C=O (X = Cl, H, and CH₃) at 298.15 K and 1 atm^a

X		step 1		step 2		
		RC → TS1	RC → INT	INT → TS2	INT → PC	RC → PC
CH ₃	ΔE	9.74	-10.10	17.83	-18.47	-28.57
	ΔE_{ZPV}	10.97	-6.67	16.78	-20.68	-27.35
	ΔH	9.90	-8.00	16.78	-19.30	-27.30
	ΔG	12.50	-4.63	16.60	-23.22	-27.85
	H	ΔE	10.56	-18.77	20.95	-8.40
ΔE_{ZPV}		11.56	-14.52	19.76	-10.86	-25.38
ΔH		10.63	-16.10	19.71	-9.52	-25.63
ΔG		13.04	-11.98	19.70	-13.06	-25.04
Cl		ΔE	22.60	-21.04	32.38	-6.20
	ΔE_{ZPV}	24.20	-16.63	31.03	-8.65	-25.28
	ΔH	22.77	-18.31	30.90	-7.39	-25.70
	ΔG	22.24	-13.52	31.78	-10.63	-24.15

^a ΔE , ΔE_{ZPV} , ΔH , and ΔG are in kilocalories per mole.

and 0.018 Å, respectively, when three H atoms are replaced with three Cl atoms. When X = CH₃, the substituted system has longer distances for the P₍₁₎-N₍₂₎, N₍₂₎-C₍₃₎, and P₍₁₎-O₍₄₎ bonds.

Table 2 reports the changes in electronic energies (ΔE), zero-point vibration energies (ΔE_{ZPV}), enthalpies (ΔH), and Gibbs free energies (ΔG) for two elementary steps of the aza-Wittig reaction X₃P=NH + H₂CO (X = CH₃, H, and Cl). The thermodynamic data were calculated using the MP2/6-31G** method at 298.15 K and 1 atm. For step 1 of the aza-Wittig reaction, the activation energy increases in the following order: CH₃ (10.97 kcal/mol) < H (11.56 kcal/mol) < Cl (24.20 kcal/mol). The activation energy of step 2 agrees with this order: CH₃ (16.78 kcal/mol) < H (19.76 kcal/mol) < Cl (31.03

kcal/mol). Thus, with regard to the parent compound, the methylation stabilizes the transition states (TS1 and TS2) by only 0.6 and 3.0 kcal/mol, respectively, whereas the chloro substituent destabilizes the two transition states by 12.6 and 11.3 kcal/mol, respectively. From Table 2, it is found that step 1 and step 2 of the aza-Wittig reaction when X = CH₃, H, and Cl are all exothermic processes. The total free energy changes are -27.85, -25.04, and -24.15 kcal/mol for CH₃, H, and Cl, respectively. So the thermodynamic effects on the equilibrium caused by the substituents are almost negligible.

The theoretical investigation has shown that the Wittig reaction of H₃P=CH₂ with H₂CO can proceed very easily due to the polar characters of the reactants.²⁶ H₃P=NH is an isoelectronic compound of H₃P=CH₂. Its increasing level of polarization should also be responsible for the destabilization of reactants in the aza-Wittig reaction of H₃P=NH and H₂CO. The stronger polarities of H₃P=NH and (CH₃)₃P=NH with dipole moments of 3.555 and 4.058 D, respectively, compared to that of Cl₃P=NH (1.436 D), suggest that the exchange of =NH in X₃P=NH and =O in H₂C=O is easier when X = H and CH₃ than when X = Cl. The atomic and group charges and their changes computed by the CHELPG method from the reactant complex to transition state TS1 and to intermediates when X = CH₃, H, and Cl are shown in Table 3. The reactant complex has a positive charge on the X₃P group and a negative charge on the NH group for three compounds. In TS1, the charge on the H₃P group becomes more positive, suggesting that the rate should increase when a stronger electron-donating group is substituted on the P₍₁₎ atom. Therefore, the aza-Wittig reaction X₃P=NH + H₂CO may be much more favorable for CH₃ than for Cl, even though the reaction energies are comparable.

TABLE 3: CHELPG Charges of the Reactant Complex and Changes in Charges Δq^\ddagger and Δq° Involved in Step 1 of the Aza-Wittig Reaction of $X_3P=NH$ with $H_2C=O$ ($X = CH_3, H,$ and Cl) at the MP2/6-31G Level of Theory (in electronic charge units)^a**

X		X_3P	NH	CH_2	O
CH ₃	q^{RC}	0.654	-0.633	0.415	-0.436
	Δq^\ddagger	0.167	0.114	0.016	-0.296
	Δq°	0.046	0.107	0.109	-0.261
H	q^{RC}	0.574	-0.541	0.418	-0.450
	Δq^\ddagger	0.006	0.106	0.010	-0.123
	Δq°	0.013	0.092	0.102	-0.208
Cl	q^{RC}	0.333	-0.316	0.411	-0.428
	Δq^\ddagger	-0.051	0.076	0.042	-0.068
	Δq°	-0.169	0.137	0.085	-0.052

^a $\Delta q^\ddagger = q^{TS1} - q^{RC}$, and $\Delta q^\circ = q^{INT} - q^{RC}$.

To analyze the substituent effects on the aza-Wittig reaction, it is necessary to understand how substituents alter the reaction energies and influence the transition state energies. One useful approach is to use Marcus theory,²⁷ which was used to analyze the activation energies of reaction pathways.²⁸ The Marcus equation is given in eq 3.

$$\Delta G^\ddagger = \Delta G_0^\ddagger + \frac{1}{2}\Delta G^\circ + (\Delta G^\circ)^2/(16\Delta G_0^\ddagger) \quad (3)$$

where ΔG_0^\ddagger is the intrinsic barrier, representing the barrier of a thermoneutral reaction. ΔG^\ddagger and ΔG° are Gibbs free energy changes of activation and reaction of a nondegenerate reaction, respectively. The third term $(\Delta G^\circ)^2/(16\Delta G_0^\ddagger)$ is the correction factor for nonadditivity of the intrinsic and thermodynamic effects. Murdoch advocated that the similar expression in eq 4 be applied to the nondegenerate reaction and applied it to some pericyclic reactions and other chemical processes.^{29,30}

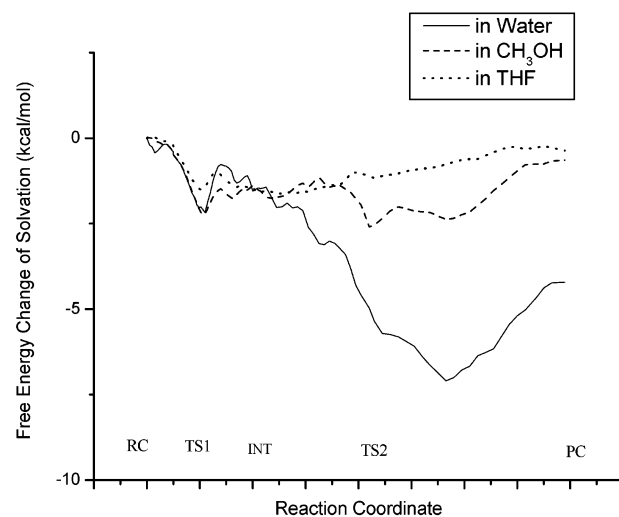
$$\Delta E^\ddagger = \Delta E_0^\ddagger + \frac{1}{2}\Delta E^\circ + (\Delta E^\circ)^2/(16\Delta E_0^\ddagger) \quad (4)$$

In this study, we used eq 4 to separate the intrinsic and thermodynamic contribution of substituent effects on the activation energy of step 1 and step 2 of the $X_3P=NH + H_2CO$ ($X = CH_3, H,$ and Cl) reaction. The intrinsic barrier, ΔE_0^\ddagger , is calculated using eq 4 with the quantum mechanically calculated values of activation energy, ΔE^\ddagger , and reaction energy, ΔE° . Table 4 shows the intrinsic barriers and thermodynamic contributions for $X_3P=NH + H_2CO$ ($X = CH_3, H,$ and Cl) reaction systems. The intrinsic activation energies of step 1 and step 2 of the parent reaction are 18.77 and 24.97 kcal/mol, respectively. For step 1, the 12.04 kcal/mol increase in the activation energy caused by three Cl atoms is mainly due to the intrinsic factor. There is a 13.49 kcal/mol increase in the intrinsic barrier, with an only 1.45 kcal/mol increase in exothermicity by these groups. For the $X = CH_3$ system, the comparable and opposite contributions of intrinsic (-4.43 kcal/mol) and thermodynamic (3.60 kcal/mol) lead to a small decrease in the activation energy of step 1. For step 2, the

TABLE 4: Activation Energies (ΔE^\ddagger), Reaction Energies (ΔE°), Intrinsic Barrier (ΔE_0^\ddagger), and Thermodynamic ($\Delta E_{thermo}^\ddagger$) Contributions as Well as Their Relative Value to the Parent Compound for Step 1 and Step 2 of the Reaction of $X_3P=NH$ with CO ($X = CH_3, H,$ and Cl) (in kilocalories per mole)^a

	X	ΔE^\ddagger	ΔE°	ΔE_0^\ddagger	$\Delta E_{thermo}^\ddagger$
step 1	CH ₃	9.74 (-0.82)	-10.10 (8.67)	14.34 (-4.43)	-4.61 (3.60)
	H	10.56 (0.00)	-18.77 (0.00)	18.77 (0.00)	-8.21 (0.00)
	Cl	22.60 (12.04)	-21.04 (-2.27)	32.26 (13.49)	-9.66 (-1.45)
step 2	CH ₃	17.83 (-3.12)	-18.47 (-10.07)	26.25 (1.28)	-8.42 (-4.40)
	H	20.95 (0.00)	-8.40 (0.00)	24.97 (0.00)	-4.02 (0.00)
	Cl	32.38 (11.43)	-6.20 (2.20)	35.41 (10.44)	-3.03 (0.99)

^a Values relative to the parent compound are shown in parentheses.

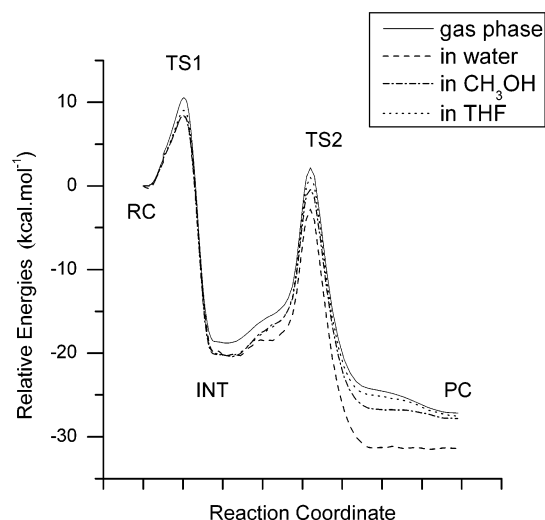
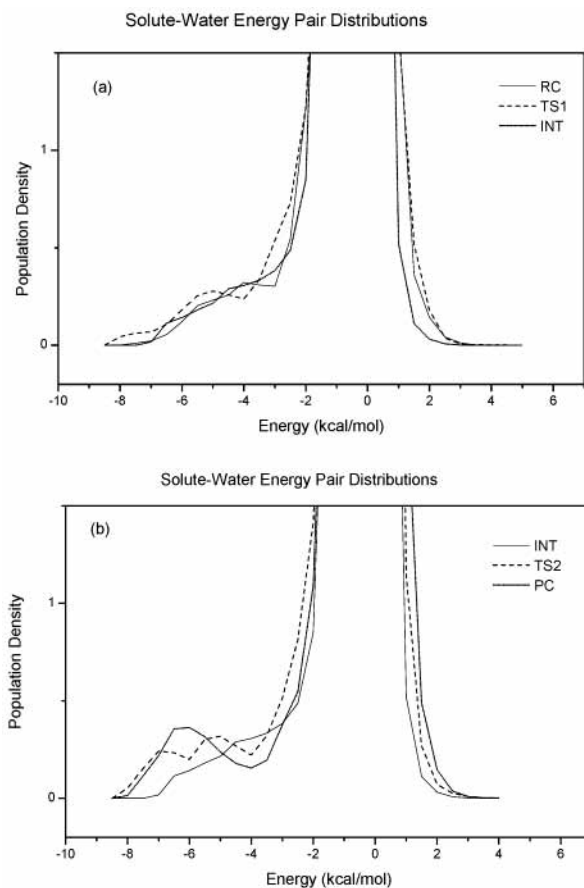
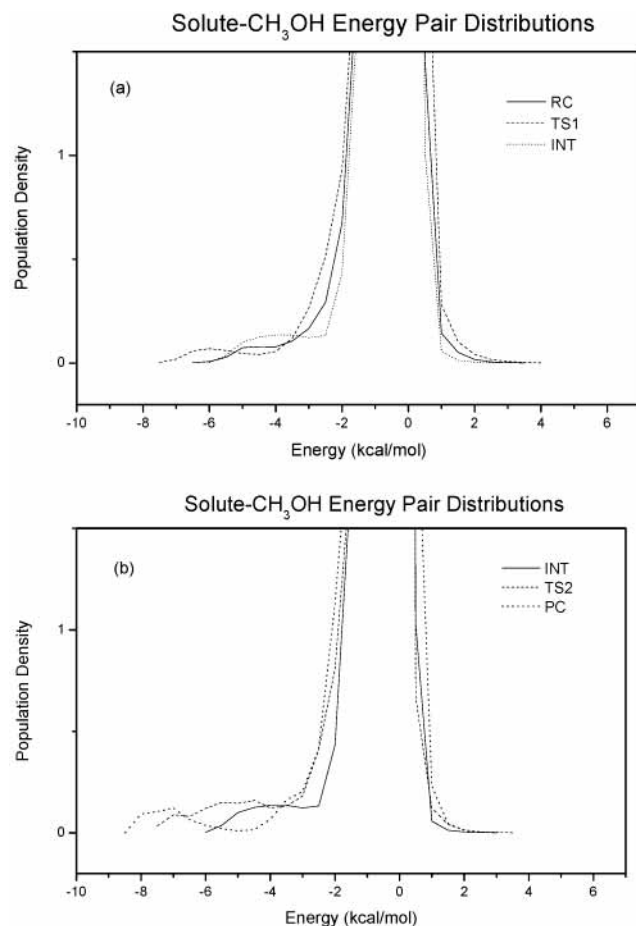
**Figure 1.** Changes in the free energies of solvation along the reaction coordinate calculated from Monte Carlo simulations.

intrinsic contribution is also a dominant factor in the activation energy increase in the $X = Cl$ system. The CH_3 group increases the exothermicity of the reaction by 10.07 kcal/mol, and most of the reduction of the activation energy comes from this effect.

3.2. Solvent Effects As Determined by Monte Carlo Simulation. The reaction of $H_3P=NH$ with formaldehyde was studied in water, CH_3OH , and THF using the free energy perturbation method implemented in BOSS 4.2.²⁴ Figure 1 displays the changes in the free energies of solvation over the course of the reaction in three solvents: water, CH_3OH , and THF. The changes in the free energies of solvation and free energy changes in the gas phase and in solution for the activation and reaction procedures of step 1 and step 2 are listed in Table 5. For step 1, the free energies of solvation decrease monotonically from RC to TS1 and then increase slightly from TS1 to INT. The differences in the free energies of solvation between RC and TS1 in water, methanol, and THF are -2.01, -2.17, and -1.50 kcal/mol, respectively, which indicates that transition state TS1 is stabilized in three solvents by solvation compared with RC. The group charges on the H_3P group and O change from 0.574 to 0.580 e and from -0.450 to -0.573 e on going from RC to TS1, respectively, enhancing the electrostatic interaction with solvents. Note that the free energy of solvation is largest in methanol even though the difference is marginal (0.16 kcal/mol) compared with that in water, suggesting that the protic polar solvents are more suitable for the aza-Wittig reaction. For step 2, TS2 is also stabilized more by solvation than INT in water and methanol, and has free energies of solvation 2.94 and 2.60 kcal/mol smaller than those of INT, respectively. On the contrary, the free energy of solvation of TS2 in THF is 0.47 kcal/mol higher than that of INT, and thus, TS2 is destabilized slightly by solvation compared with INT in THF.

TABLE 5: Changes in the Free Energies of Solvation (ΔG_{sol}) and Total Free Energy Differences (ΔG_{tot}) in the Gas Phase and Solutions for Step 1 and Step 2 of the Reaction of $\text{H}_3\text{P}=\text{NH}$ with H_2CO (in kilocalories per mole)

solvent	$\Delta G_{1,\text{sol}}^\ddagger$	$\Delta G_{1,\text{sol}}^\circ$	$\Delta G_{2,\text{sol}}^\ddagger$	$\Delta G_{2,\text{sol}}^\circ$	$\Delta G_{1,\text{tot}}^\ddagger$	$\Delta G_{1,\text{tot}}^\circ$	$\Delta G_{2,\text{tot}}^\ddagger$	$\Delta G_{2,\text{tot}}^\circ$
gas phase					13.04	-11.98	19.70	-13.06
water	-2.01	-2.03	-2.94	-2.99	11.03	-14.01	16.76	-16.05
CH_3OH	-2.17	-1.51	-2.60	0.87	10.87	-13.49	18.11	-12.19
THF	-1.50	-1.60	0.47	1.24	11.54	-13.58	20.17	-11.82

**Figure 2.** Minimum energy path $E_{\text{MEP}}(s)$ for the aza-Wittig reaction of $\text{H}_3\text{P}=\text{NH}$ with $\text{H}_2\text{C}=\text{O}$ in the gas phase and in three solvents (water, CH_3OH , and THF).**Figure 3.** Energy pair distributions of the solute-water interaction for RC, TS1, and INT (a) and for INT, TS2, and PC (b). The ordinate gives the number of water molecules coordinated with the solute with the interaction energy shown on the abscissa. The units for the y-axis are the number of molecules per kilocalorie per mole.**Figure 4.** Energy pair distributions of the solute- CH_3OH interaction for RC, TS1, and INT (a) and for INT, TS2, and PC (b). The ordinate gives the number of THF molecules coordinated with the solute with the interaction energy shown on the abscissa. The units for the y-axis are the number of molecules per kilocalorie per mole.

For an aqueous solution, the calculated free energies of activation of step 1 and step 2 by combining *ab initio* MO calculation (the MP2/6-31G** level) with Monte Carlo simulation are 11.03 and 16.76 kcal/mol, respectively, which are close to the results obtained by the SCRf (PCM model) method,²⁰ where the free energies of activation are 10.94 and 18.27 kcal/mol, respectively. The free energy changes of reaction for step 1 and step 2 are -14.01 and -16.05 kcal/mol, respectively, and are also consistent with the SCRf results with the free energy changes of reaction of -13.94 and -16.19 kcal/mol, respectively. Figure 2 depicts the relative potential energy profiles $E_{\text{MEP}}(s)$ along the minimum energy path (MEP) in the gas phase and in three solvents (water, methanol, and THF). From Table 5 and Figure 2, the solvent effects on the $\text{H}_3\text{P}=\text{NH} + \text{H}_2\text{CO}$ reaction of water and methanol are computed to be more favorable than that in THF.

Figures 3-5 show the solute-solvent energy pair distributions for RC, TS1, INT, TS2, and PC of the $\text{H}_3\text{P}=\text{NH} + \text{H}_2\text{CO}$ system in water, CH_3OH , and THF, respectively. The plots give the number of solvent molecules on the ordinate that

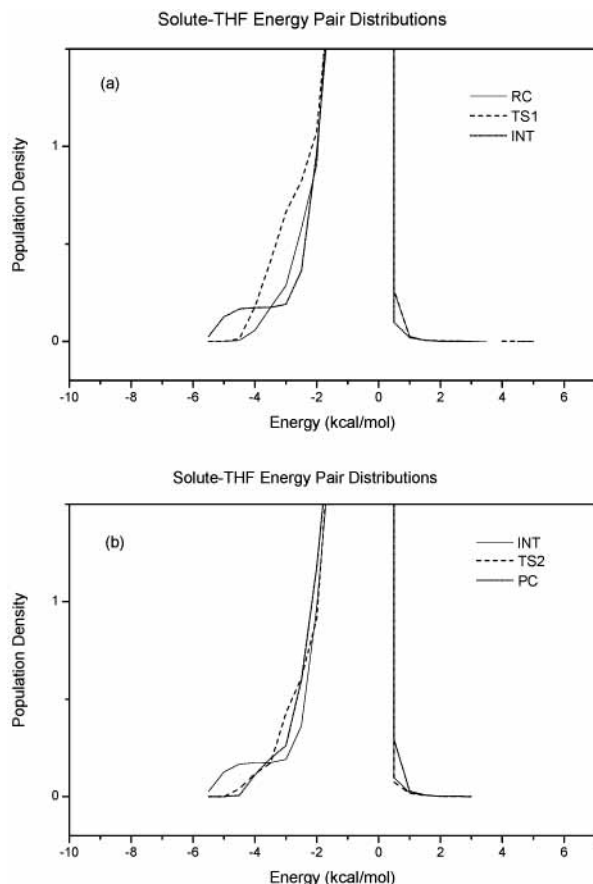


Figure 5. Energy pair distributions of the solute-THF interaction for RC, TS1, and INT (a) and for INT, TS2, and PC (b). The ordinate gives the number of THF molecules coordinated with the solute with the interaction energy shown on the abscissa. The units for the y-axis are the number of molecules per kilocalorie per mole.

interact with the solute with the interaction energy shown on the abscissa. In three solvents, the spikes centered at 0.0 kcal/mol result from the weak interactions between the solute and many distant solvent molecules. From Figure 3, for RC in water, there is a bound group of solvent molecules, which forms a band from ca. -8.0 to -2.5 kcal/mol. Integration of the distribution curve for RC up to the end of this band at -2.5 kcal/mol defines 1.54 water molecules that interact with solute. Integration of the curves for TS1, INT, TS2, and PC until this limit results in 3.12, 2.47, 3.65, and 3.08 water molecules, respectively. In CH_3OH and THF, integration of the curves up to the end of the plateaus at -2.5 kcal/mol reveals 1.51, 2.85, 2.22, 2.80, and 2.76 CH_3OH molecules and 1.10, 2.09, 1.22, 1.17, and 1.12 THF molecules for these structures as shown in Figures 4 and 5, respectively. For step 1, the numbers of water and methanol molecules strongly interacting with solute increase by 1.58 and 1.34, respectively, on going from RC to TS1, while the change is only 0.99 in THF. For step 2, from INT to TS2, the increasing numbers of water and methanol molecules are 1.18 and 0.58, respectively, and the corresponding number in THF is -0.05 . These differences imply that the stabilization of the transition structure relative to its reactant is different in water, methanol, and THF. In water and methanol, the better solvation of the TS can be attributed to a larger increase in the extent of interaction between solute and solvent molecules, while in THF, the changes for the interactions with the solvent along the reaction path are smaller or even negative.

4. Conclusion

The title aza-Wittig reactions of $\text{X}_3\text{P}=\text{NH}$ with $\text{H}_2\text{C}=\text{O}$ were studied using the *ab initio* MP2/6-31G** level of theory. The electron-donating CH_3 groups at the P atom accelerate slightly two elementary steps of this reaction. In contrast, the electron-withdrawing Cl substituents at the P atom largely increase the activation barriers of two steps. Obviously, the aza-Wittig reaction of $\text{X}_3\text{P}=\text{NH}$ with $\text{H}_2\text{C}=\text{O}$ can proceed more favorably when $\text{X} = \text{CH}_3$ and H than when $\text{X} = \text{Cl}$ in the gas phase. The effect of substituents on the shift of the total equilibrium of this reaction is negligible.

Relative free energies of solvation to the reactant complex along the reaction path were calculated using the free energy perturbation method implemented in Monte Carlo simulations. In water and CH_3OH , two transition states (TS1 and TS2) of the aza-Wittig reaction were stabilized by solvation. THF stabilizes transition state TS1 and destabilizes transition state TS2 slightly. Solute-solvent energy pair distribution analysis indicates that one to three solvent molecules are in strong interaction with the solute. The calculated values correctly reflect the fact that the effects of water and CH_3OH are more favorable than that of THF.

Acknowledgment. This work was supported by Korea Research Foundation Grant KRF-2000-015-DP0208.

References and Notes

- (1) Lischka, H. *J. Am. Chem. Soc.* **1977**, *99*, 353.
- (2) Holler, R.; Lischka, H. *J. Am. Chem. Soc.* **1980**, *102*, 4632.
- (3) Eades, R. A.; Gassman, P. G.; Dixon, D. A. *J. Am. Chem. Soc.* **1981**, *103*, 1066.
- (4) Vincent, M. A.; Schaefer, H. F., III; Schier, A.; Schmidbaur, H. *J. Am. Chem. Soc.* **1983**, *105*, 3806.
- (5) Dixon, D. A.; Smart, B. E. *J. Am. Chem. Soc.* **1986**, *108*, 7172.
- (6) Volatron, F.; Einstein, O. *J. Am. Chem. Soc.* **1987**, *109*, 1.
- (7) Nguyen, M. T.; Hegarty, A. F. *J. Chem. Soc., Perkin Trans. 2* **1987**, 47.
- (8) Streitwieser, A.; Rajca, A.; McDowell, R. S.; Glaser, R. J. *J. Am. Chem. Soc.* **1987**, *109*, 4184.
- (9) Bachrach, S. M. *J. Org. Chem.* **1992**, *57*, 4367.
- (10) Naito, T.; Nagase, S.; Yamataka, H. *J. Am. Chem. Soc.* **1994**, *116*, 10080.
- (11) Gololobov, Y. G.; Zhmurova, I. N.; Kasukhin, L. F. *Tetrahedron* **1981**, *43*, 437.
- (12) Mathis, R.; Zenati, N.; Ayed, N.; Sanchez, M. *Spectrosc. Chim. Acta* **1982**, *38A*, 1181.
- (13) Eric, F. V. S.; Kenneth, T. *Chem. Rev.* **1988**, *88*, 297.
- (14) Gololobov, Y. G.; Kasukhin, L. F. *Tetrahedron* **1992**, *48*, 1406.
- (15) Johnson, A. W. *Ylides and Imines of Phosphorus*; John Wiley & Sons: New York, 1993.
- (16) Gonbeau, D.; Pfister-Guillouzo, G.; Mazieres, M.-R.; Sanchez, M. *Can. J. Chem.* **1985**, *63*, 3242.
- (17) Sudhakar, V.; Lammertsma, K. *J. Am. Chem. Soc.* **1991**, *113*, 1899.
- (18) Koketsu, J.; Ninomiya, Y.; Suzuki, Y.; Koga, N. *Inorg. Chem.* **1997**, *36*, 694.
- (19) Lu, W. C.; Sun, Ch. Ch.; Zang, Q. J.; Liu, Ch. B. *Chem. Phys. Lett.* **1999**, *311*, 491.
- (20) Xue, Y.; Xie, D.; Yan, G. *J. Phys. Chem. A* **2002**, *106*, 9053.
- (21) Fukui, K. *J. Phys. Chem.* **1970**, *74*, 4161.
- (22) Breneman, C. M.; Wiberg, K. B. *J. Comput. Chem.* **1990**, *11*, 361.
- (23) Frisch, M. J.; Trucks, G. W.; Schlegel, H. B.; Scuseria, G. E.; Robb, M. A.; Cheeseman, J. R.; Zakrzewski, V. G.; Montgomery, J. A., Jr.; Stratmann, R. E.; Burant, J. C.; Dapprich, S.; Millam, J. M.; Daniels, A. D.; Kudin, K. N.; Strain, M. C.; Farkas, O.; Tomasi, J.; Barone, V.; Cossi, M.; Cammi, R.; Mennucci, B.; Pomelli, C.; Adamo, C.; Clifford, S.; Ochterski, J.; Petersson, G. A.; Ayala, P. Y.; Cui, Q.; Morokuma, K.; Malick, D. K.; Rabuck, A. D.; Raghavachari, K.; Foresman, J. B.; Cioslowski, J.; Ortiz, J. V.; Stefanov, B. B.; Liu, G.; Liashenko, A.; Piskorz, P.; Komaromi, I.; Gomperts, R.; Martin, R. L.; Fox, D. J.; Keith, T.; Al-Laham, M. A.; Peng, C. Y.; Nanayakkara, A.; Gonzalez, C.; Challacombe, M.; Gill, P. M.

W.; Johnson, B.; Chen, W.; Wong, M. W.; Andres, J. L.; Gonzalez, C.; Head-Gordon, M.; Replogle, E. S.; Pople, J. A. *Gaussian 98*, revision A.7; Gaussian Inc.: Pittsburgh, PA, 1998.

(24) Jorgensen, W. L. *BOSS*, version 4.2; Yale University: New Haven, CT.

(25) Jorgensen, W. L.; Ravimohan, C. *J. Chem. Phys.* **1985**, 83, 3050.

(26) Naito, T.; Nagase, S.; Yamataka, H. *J. Am. Chem. Soc.* **1994**, 116, 10080.

(27) Marcus, R. A. *J. Chem. Phys.* **1956**, 24, 966.

(28) Yoo, H. Y.; Houk, K. N. *J. Am. Chem. Soc.* **1997**, 119, 2877.

(29) Murdoch, J. R. *J. Am. Chem. Soc.* **1983**, 105, 2660.

(30) Murdoch, J. R. *J. Am. Chem. Soc.* **1983**, 105, 2159